Positronium

Vanessa Cerrone
Matr. 2053044

Sabrina Ciarlantini
Matr. 2054770

Aurora Leso
Matr. 2055703

03/04/08 November 2021

---

1 Aims of the experiment

1. Measuring the **branching ratio between the two and three photons decay** of the Positronium.
2. Measuring the **lifetime of the Positronium** studying the time distribution of the decays.

2 Introduction

The Positronium is a bound state of a positron and an electron and it can be created as a consequence of a β decay, hence with the emission of a positron. The latter can then annihilate with an electron in multiple ways, depending on how their spins are coupled together, emitting a different number of photons. Within the context of this report, a source of ^{22}**Na** , with an activity of around 380 kBq, has been employed: it decays β^+ into an excited state of ^{22}**Ne**, which then emits (within few picoseconds) a 1275 keV gamma ray.

Two types of decay have been studied and observed: two and three photons (**2γ** and **3γ**).

- The **2γ** decay is the most probable and corresponds to the coupling of spins at S=0, which means the state is a singlet, called **para-Positronium**. Due to momentum and energy conservation, each photon carries an energy of 511 keV, following trajectories with opposite directions.
- The **3γ** decay, which is less probable (ratio of 1 to 137 with respect to the para-Positronium decay), corresponds to the coupling of spins at S=1, so in a triplet state called **ortho-Positronium**.

3 Experimental setup

In this section, the description of the experimental setup is provided.

- **Detectors**: four NaI(Tl) inorganic scintillators have been used during the experience. From now on they will be addressed as D1, D2, D3, and D4. The first three are coplanar: D2 and D3 have a fixed angle of θ_{23}=120°, whereas D1 is on a movable arm which allows to modify the value of θ_{12} and θ_{13}. D4 is instead positioned vertically above the source, out of the plane. The detectors are positioned with their ends against a lead shielding, with the purpose of minimizing the probability for a gamma ray to scatter off one detector and interact with another one.
- **Photomultipliers** (PMTs): they are the XP2020 PMTs supplied by Philips. They are connected to the CAEN N472 power supply, which guarantees the appropriated High Voltage (HV).
- **Fan-In Fan-Out**: this module allows to replicate the input signal, preserving its shape.

- **Constant Fraction Timing Discriminator (CFTD)**: this module fixes problems arising from the identification of the exact time an event occurs, so the moment in which a particle interacts with the scintillator.
- **Coincidence Unit**
- **Time To Amplitude Converter (TAC)** : this module produces as output a voltage signal proportional to the time interval between the START and STOP signals.
- **Oscilloscope**: Tektronix TBS1102B.
- **Acquisition System (DAQ)**: the acquisition system used in the experience is called VERDI and it acquires directly from the CAEN DT5720 digitizer, with four channels, a sampling rate of 250 Ms/s and a resolution of 12 bits.

3.1 Preliminary signal analysis

Analog signals coming from the detectors are processed through different steps of an electronics chain, which will be described in following sections. A preliminary analysis was needed in order to set the CFTD threshold to a proper value that would minimize the background noise. In Figure 1, the signals visualized on the oscilloscope display are reported.

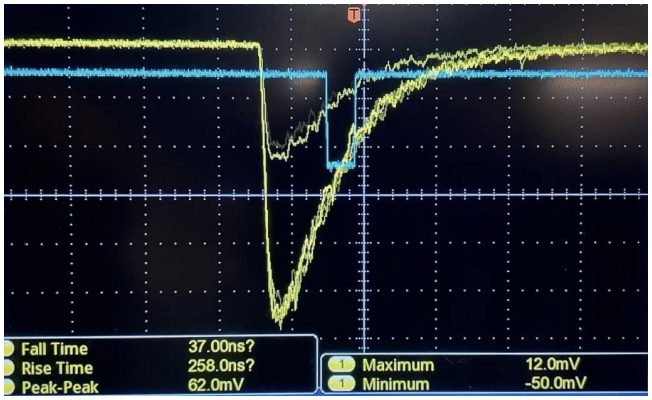

Figure 1: Oscilloscope display: in blue the trigger signal from the delayed CFTD output of D1. In yellow the anode signal from the same detector; both peaks, at 511 keV ($\sim$ 100 mV) and at 1275 keV ($\sim$ 280 mV) are visible.

For D1, D2 and D3 the threshold value has been fixed just above the electronics noise. For D4 a higher value has been set in order to see only the most energetic peak at 1275 keV.

4 Calibration

4.1 Energy calibration

In order to find the energy calibration of the detectors, the following linear function has been used:

$$E[\text{keV}] = \alpha + \beta \cdot \text{ADC} \tag{1}$$

where the expected peak energy values have been taken from LNHB[1] website. Since the background before and after each peak appears variable, to fit the peaks a gaussian plus a linear background is used:

$$f(x) = a + b \cdot x + \text{N} \cdot e^{-\frac{(x-\mu)^2}{2\sigma^2}} \tag{2}$$

Since there are only two visible peaks, it has to be taken into account that the calibration is approximate, even if its results are functional for this report aims.

[1]Laboratoire National Henri Becquerel, `http://www.lnhb.fr`

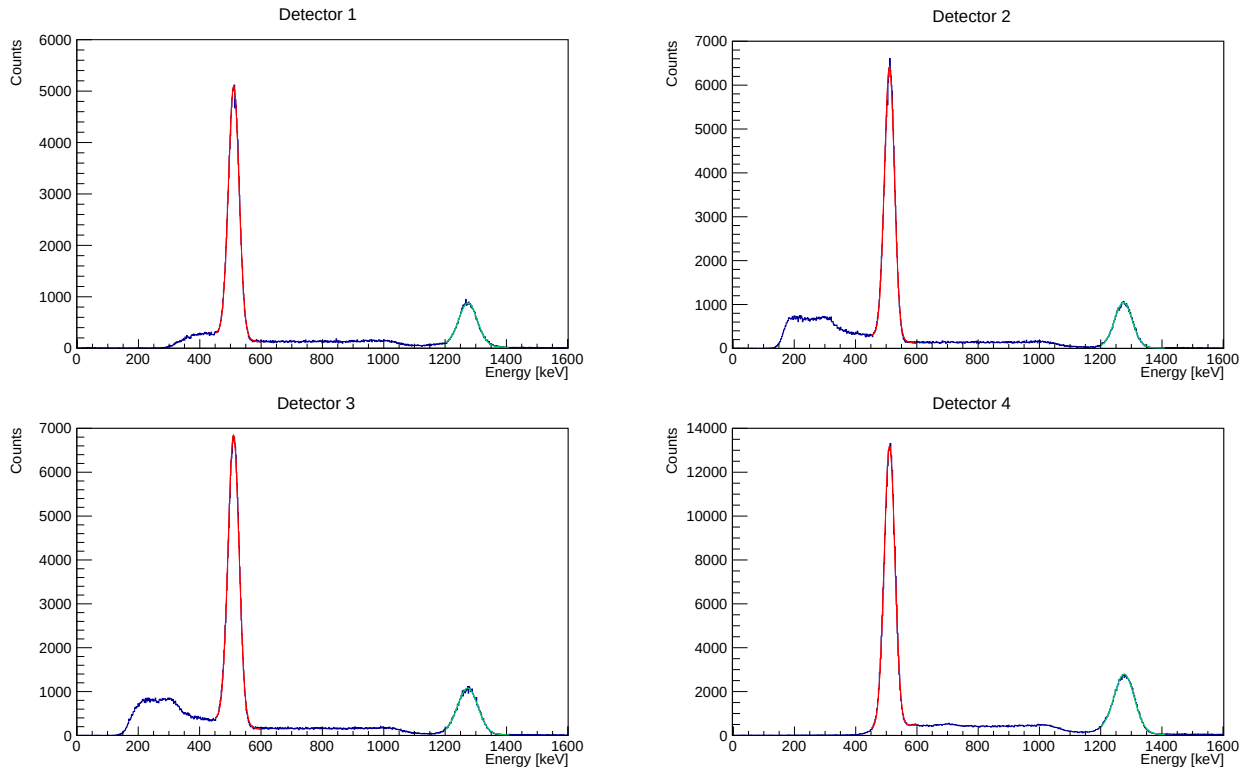

Figure 2: Detectors calibrated spectra. Gaussian + linear background fit is shown both on the 511 keV and on the 1275 keV peaks. Notice the higher value of the threshold set for D1 and D4.

The graphs in Figure 2 show the calibrated spectra, obtained following the procedure aforementioned and the results of the linear regressions for the 4 detectors have been collected in Table 1.

Detector	α [keV]	β [keV/ADC counts]
D1	-18 ± 2	0.1157 ± 0.0002
D2	-22 ± 2	0.1144 ± 0.0002
D3	-23 ± 2	0.1104 ± 0.0002
D4	-34 ± 2	0.1817 ± 0.0003

Table 1: Results of the linear regressions for the 4 detectors.

In the following tables, the results of the gaussian fits are reported: Table 2 shows the mean values and standard deviations for the non-calibrated spectra, while Table 3 shows the same parameters but for the calibrated ones. In particular, from the latter, one can infer that the energy calibration works well, given that there's a good agreement between experimental and theoretical values.

Detector	μ_1 [ADC counts]	σ_1 [ADC counts]	μ_2 [ADC counts]	σ_2 [ADC counts]
D1	4571.5 ± 0.5	151.0 ± 0.5	11178 ± 2	259 ± 2
D2	4657.4 ± 0.4	143.7 ± 0.4	11337 ± 2	258 ± 2
D3	4839.9 ± 0.5	167.1 ± 0.6	11760 ± 2	310 ± 2
D4	2996 ± 1	105 ± 1	7192 ± 1	227 ± 1

Table 2: Energy calibration data: results of gaussian fit for non-calibrated spectra. The two peaks, at 511 keV and 1275 keV, are indexed as 1 and 2 respectively.

Moreover, the resolution of the four detectors has been computed as:

$$R = \frac{\text{FWHM [keV]}}{\mu\text{[keV]}}$$

Detector	μ_1 [keV]	σ_1 [keV]	R_1	μ_2 [keV]	σ_2 [keV]	R_2
D1	510.77 ± 0.06	17.38 ± 0.06	8.0%	1274.8 ± 0.2	30.5 ± 0.3	5.6%
D2	510.72 ± 0.05	16.27 ± 0.05	7.5%	1274.1 ± 0.2	28.8 ± 0.2	5.3%
D3	510.66 ± 0.05	17.98 ± 0.05	8.3%	1274.2 ± 0.2	32.9 ± 0.3	6.1%
D4	510.19 ± 0.05	17.46 ± 0.04	8.1%	1274.7 ± 0.2	32.8 ± 0.2	6.1%

Table 3: Energy calibration data: results of gaussian fit for calibrated spectra. The two peaks, at 511 keV and 1275 keV, are indexed as 1 and 2 respectively.

The obtained resolutions of the four detectors are comparable at fixed energy and follow the expected trend, i.e. they improve as the gamma ray energy increases ($\propto 1\sqrt{E}$).

4.2 TAC calibration

In order to calibrate the TAC unit, several spectra were produced using a detector signal delayed by a chosen value, by acting on a delay unit. Just as the previous calibration, the following fit function has been used:

$$\text{Delay[ns]} = a + b \cdot \text{ADC} \tag{3}$$

where the nanoseconds values are known a priori (they are manually set), and the ADC counts values correspond to the centroid of the peaks. The results of the linear regression are:

$$a = (-0.02 \pm 0.06)\ \text{ns} \qquad b = (0.01161 \pm 0.00002)\ \text{ns/ADC counts}$$

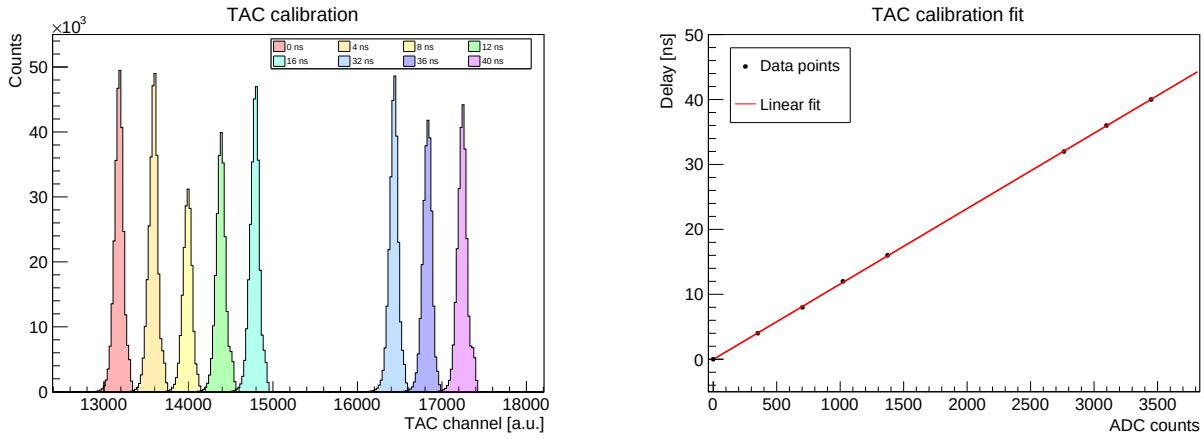

Figure 3: TAC calibration data and fit.

As it can be seen in Figure 3, the linear trend is confirmed by the experimental data without any unexpected behavior. Since the fit is obtained without considering any uncertainty on the experimental data, the errors associated to the fit parameters by the ROOT program are connected to a not weighted fit.

5 Dead time

The digitizer has an inherent dead time τ_d, i.e. the time required by the system to process one event before it is ready to process another. With the purpose of estimating the dead time, during the three experimental days multiple tests have been carried out by measuring the rate of acquired events both with the digitizer (evaluating the number of counts in the histograms over the acquisition time) and with a scaler module. The latter has a negligible dead time, so it's appropriate to use it to get an approximate value of the real counting rate of the detectors. The results are summarized in Table 4.

Detector	Rate scaler [Hz]	Measured Rate [Hz]
D1	10435	3810 ± 8
D2	12521	4959 ± 9
D3	12441	6543 ± 10
D4	6729	6541 ± 10
D1&D2	4432	3531 ± 8
D1&D2&D4	42	39.5 ± 0.8

Table 4: Real counting rate measured by the scaler module and digitizer acquisition rate (errors computed assuming Poisson distribution).

In order to have an idea of how the dead time affects the experimental results, the percentage of lost events has been plotted in function of the real counting rate measured by the scaler module.

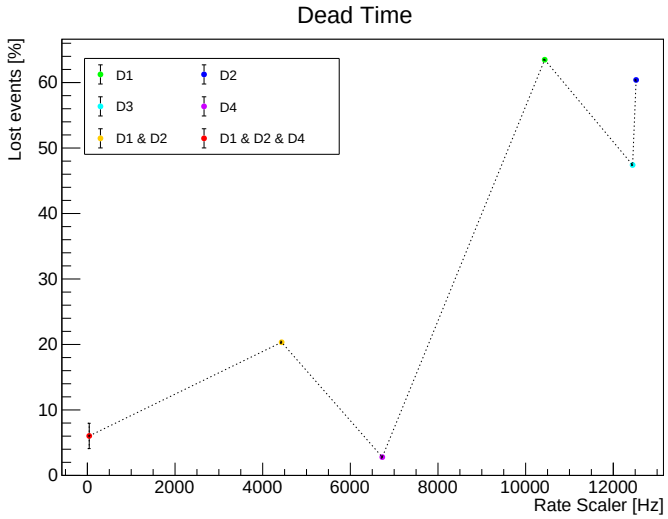

Figure 4: Lost events in function of real rate measured with the scaler module.

As it can be seen in Figure 4, the percentage of lost events increases with the rate of the incoming signal, behavior that is consistent with our expectations. Nevertheless, data do not seem to follow any specific trend, so it's not possible to provide any precise estimation of the dead time. It needs to be underlined that the result connected to the 3-photons decay has not been considered: since the events are rare, the rate is extremely low and the corrections due to the dead time should be a priori irrelevant. As a result of this shallow analysis, we deduce that the dead time correction is quite incisive for high rates (i.e. calibration data for D1, D2 and D3, where more than 50% of events got lost) while for 2γ and 3γ events (i.e. acquired triggering on the coincidence between more detectors) the reduced the counting rate makes the digitizer dead time negligible.

6 Two photons decay

In this section, the para-Positronium two photons decay is studied, analyzing both the energetic and the temporal distribution of events.

6.1 Experimental setup

To detect two photons events, the detectors have been placed as in Figure 5 on the left, i.e. in a configuration such that θ_{12}=180°, θ_{13}=120° and θ_{23}=60°. The electronics scheme that was employed to acquire this set of data is reported in the right panel of Figure 5. The anode signals from D1 and D2 have been connected to the FAN-IN-FAN-OUT and its output to channels 0 and 1 of the DAQ, respectively. The coincidence between the delayed CFTD output signals from D1, D2 and D4 has been set as a trigger for the DAQ. Moreover, the temporal distribution between the two events was measured by means of a TAC: the prompt CFTD output of D4 was used as START signal (^{22}Na decay) and the output of the coincidence unit as a STOP (positronium decay). The range of the TAC has been properly chosen in order to avoid the saturation of the Analog to Digital Converter (ADC).

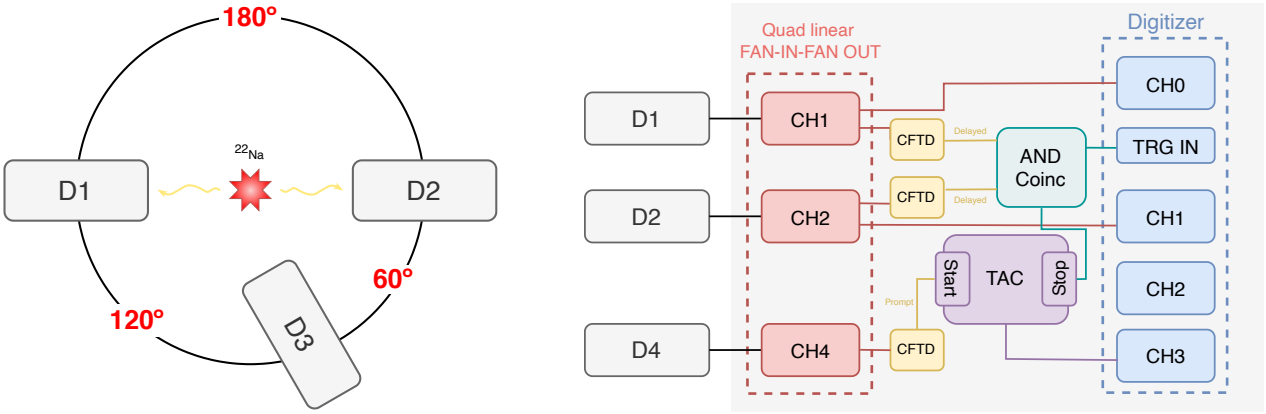

Figure 5: Two photons setup. Left: placement of coplanar detectors 1,2 and 3 (detector 4 is out of plane). Right: electronics scheme and connections.

6.2 Two gammas events

We launched a one-hour-long acquisition to have a sufficient high statistics sample: the DAQ registered 144448 events, thereby resulting in a rate of roughly 40 Hz. Raw data were processed and the energy spectra for D1 and D2 were produced. In addition to that, a filtering process has been performed: the events whose sum of the energies collected by D1 and D2 differ from the expected 1022 keV for more than 10% are discarded. Both filtered and raw spectra are shown in Figure 6. For D1 we notice a higher loss of events in the 511 keV with respect to D2: this is probably due to the different values of the thresholds that were set for the two detectors. In both cases, due to the fact that the threshold value was most likely too high, only the photo-peak and part of the compton continuum are visible. The thresholds will consequently be adjusted for future acquisitions, i.e. the three photons events in the following section.

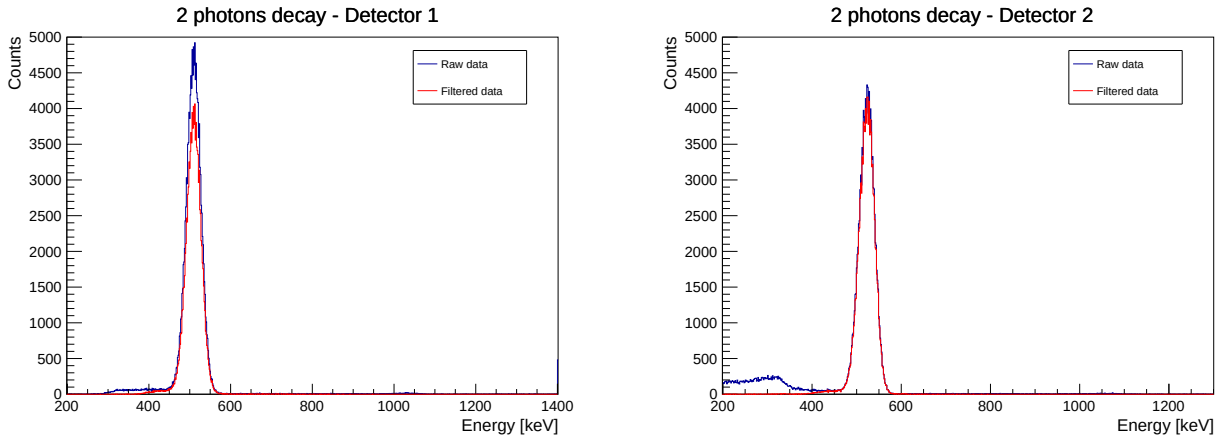

Figure 6: Left: Detector 1 spectrum. Right: detector 2 spectrum. In both panels raw data are reported in blue, whereas filtered data in red. Note the absence of the 1275 keV peak, as expected.

Additionally, the energies measured by each detector are summed and incremented in a spectrum, reported on the left panel of Figure 7. Since the centroid of the distribution is $\sim$ 1022 keV, the experimental outcome shows a good agreement with theoretical predictions.

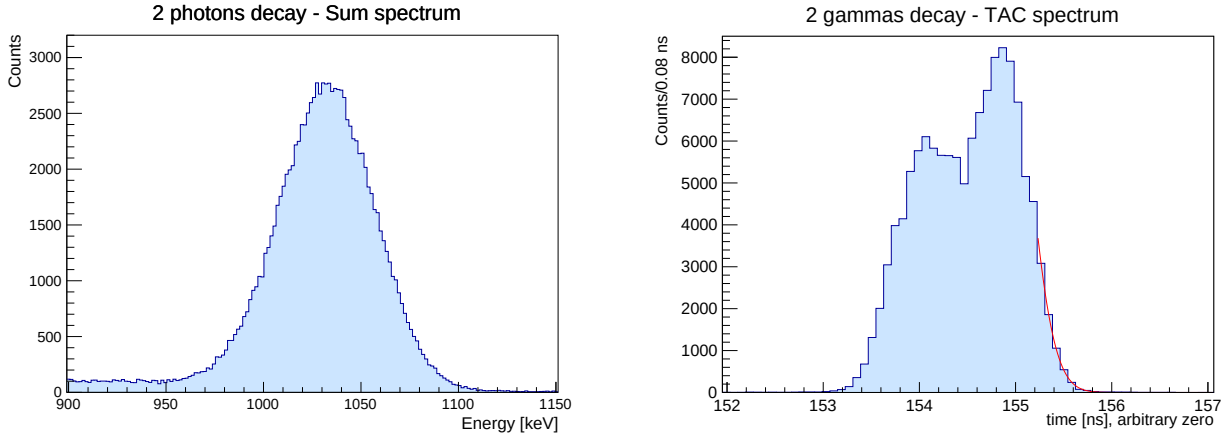

Figure 7: Left: Sum spectrum for two gammas decay. Right: TAC spectrum for two gammas decay, with exponential fit (red line).

The temporal distribution of events was studied by analyzing the acquired TAC spectrum. We established the connections as explained in Section 6.1, hence it was possible to estimate the number of events acquired after the energetic photon had been detected by D4 (signal that was indeed used as START). We obtained the spectrum reported in Figure 7 (right): we notice a peak centered at an arbitrary value, determined by the electronics and cable configuration employed. The result is the convolution of the decay law with the statistical gaussian error. Fitting the right tail, where the gaussian trend is negligible, with an exponential function in the form $f(x) = a \cdot e^{bx}$, it's possible to estimate the characteristic parameters of the decay. In particular, the mean lifetime τ is retrieved using the relation $\tau = -\frac{1}{b}$, with associated uncertainty computed by proper propagation. The following parameters are found:

$$b = (-8.207 \pm 0.001)\ \text{ns}^{-1} \implies \tau = (0.1218 \pm 0.0002)\ \text{ns}$$

Therefore, we highlight a good agreement with the expected theoretical value[2], which is 0.1244 ns.

[2]Karshenboim, Savely G. *Precision Study of Positronium: Testing Bound State QED Theory.* Int.J.Mod.Phys. A19 (2004). `arXiv:hep-ph/0310099`

7 Three photons decay

In this section, the ortho-Positronium three photons decay is studied, analyzing both the energetic and the temporal distribution of events.

7.1 Experimental setup

To detect three photons events, the detectors have been placed as in Figure 8 on the left, namely in a configuration in which $\theta_{12} = \theta_{13} = \theta_{23}$=120°. This specific choice of angles is explained by looking at the energy spectra at different angular positions of the detectors[3]; indeed, in this symmetrical configuration, the three photons are expected to be emitted with the same energy, i.e. $\sim$ 340keV, one-third of the available total energy. The electronics scheme is reported in the right panel of Figure 8. The anode signals from D1, D2 and D3 have been connected to the FAN-IN-FAN-OUT and its output to channels 0, 1 and 2 of the DAQ, respectively. The coincidence between the delayed CFTD output signals from D1, D2 and D3 has been set as a trigger for the DAQ. The optimal solution would have required to add also D4 to the coincidence unit, but this would have drastically reduced the rate of events, which is already extremely low. The temporal distribution was investigated using the TAC, as previously explained in Section 6.1.

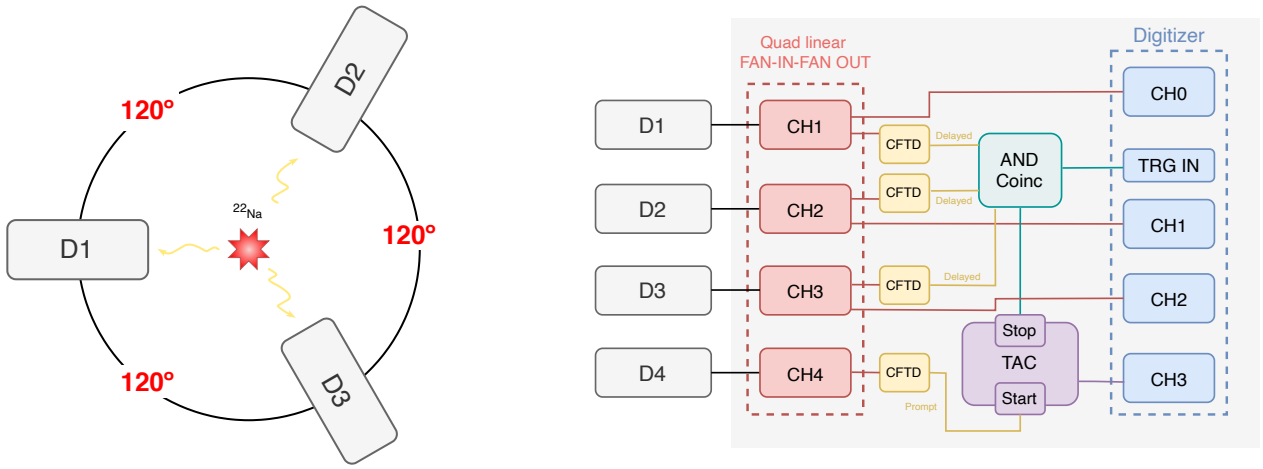

Figure 8: Three photons setup. Left: placement of coplanar detectors 1,2 and 3 (detector 4 is out of plane). Right: electronics scheme and connections.

7.2 Three gammas events

The three photons decay is a rare process, so it was necessary to launch a long run to guarantee adequate statistics: 342016 entries were acquired within a 21 hours time window. Nevertheless, it needs to be stressed that not all of them correspond to three photons events. This aspect can be discussed by examining the resulting calibrated spectra for D1, D2 and D3, reported in Figure 9. For instance, different peaks are clearly distinguishable, deriving from spurious events, e.g. a 1275 keV photon depositing its energy in one of the detectors or a back-scatter photon (see the peak at $\sim$ 80 keV). We can then deduce that there's a significant probability of having interfering false signals from scattering or multiple events that occur simultaneously.

Similarly to what was previously done, a filtering procedure was then carried out: in this case, different types of constraints, both on the energy and TAC spectra, could be potentially added in order to isolate the three photons events. As an example, one could require that the 1275 keV photon is actually detected by D4, a condition that is satisfied when the TAC signal is greater than zero. We chose to proceed in the following way:

[3]S. DeBenedetti, R. T. Siegel. *The Three-Photon Annihilation of Positrons and Electrons*

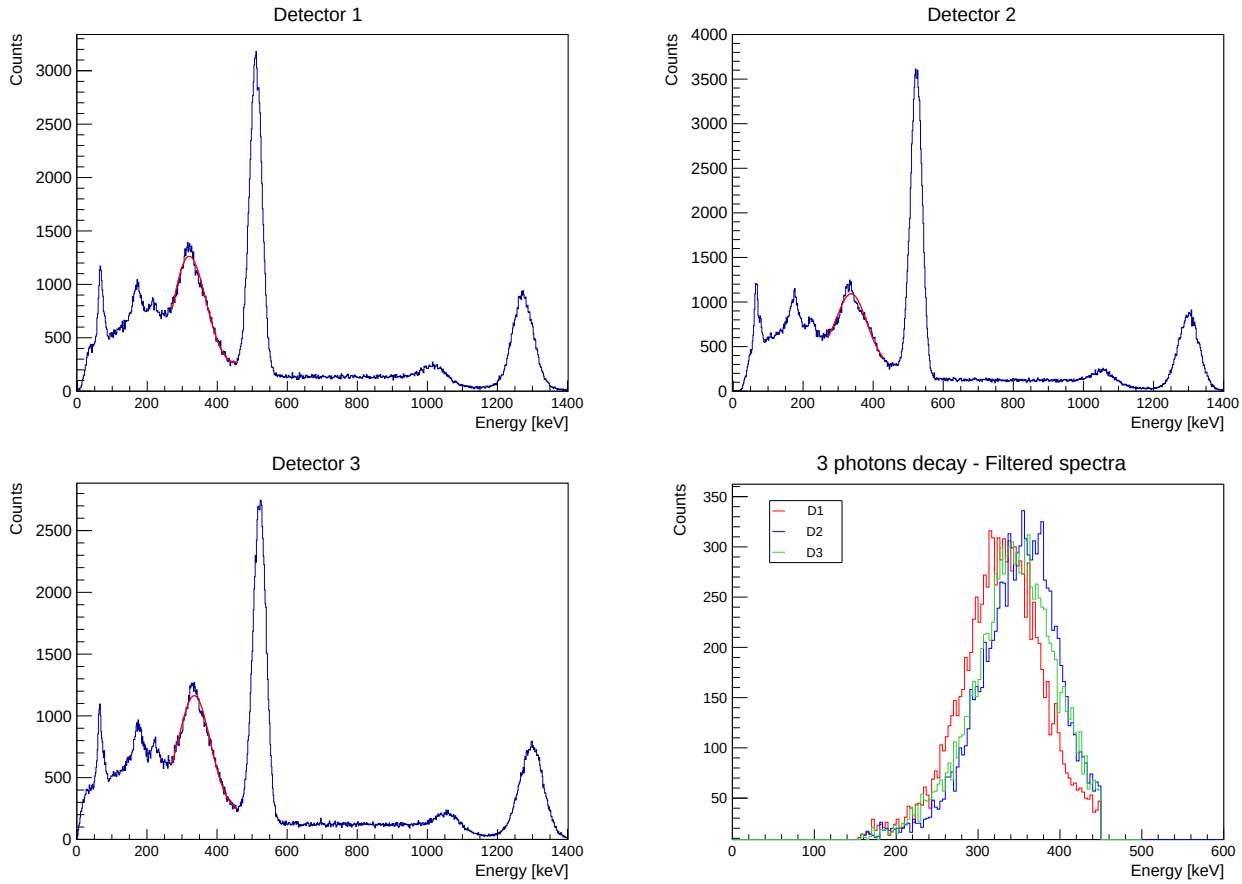

Figure 9: Detectors calibrated spectra. Last panel: filtered spectra.

1. due to the angular configuration we expect the three coplanar detectors to collect $\sim$ 340 keV each, thus the events whose sum of energies (of D1, D2 and D3) differ from 1022 keV for more than 10% are discarded. The additional restriction on the TAC signal is not included because it is needed to guarantee that the 1275 keV photon is not detected by one of the complanar detectors, a condition that is in any case satisfied;

2. for each detector only events with less than 450 keV are considered: in this way it's possible to exclude the 511 keV peak.

The resulting filtered spectra are reported in the last panel of Figure 9. The mean energy of the photon is approximately $\sim$ 340 keV, which is consistent with the geometry of the experimental setup. The number of entries turns out to be 11313, hence corresponding to a rate of roughly 0.15 Hz.
The triple coincidence configuration can be further investigated through bi-dimensional histograms, shown in Figure 10. In the first three figures, the energy E_i of one detector on the y-axis is plotted against the total energy $E_{sum} = \sum_{i=1}^{3} E_i$. The horizontal and oblique lines correspond to events in which at least one photon has fully deposited its energy while only part of the other photons' energy was collected: see for example the photopeaks at 511 keV and 1275 keV in one detector. The 2295 keV peak in the sum spectrum is a consequence of two back-to-back 511 keV photons plus the 1274 keV transition, whereas the E_{sum} =1022 keV peak is a combination of the two annihilation channels of ortho-Positronium and para-Positronium. The candidates for the three photons emission are selected as explained above, and an example of the filtered spectrum is shown in the fourth panel of Figure 10. See Figure 11 (left) for the 1D-projection of E_{sum}.

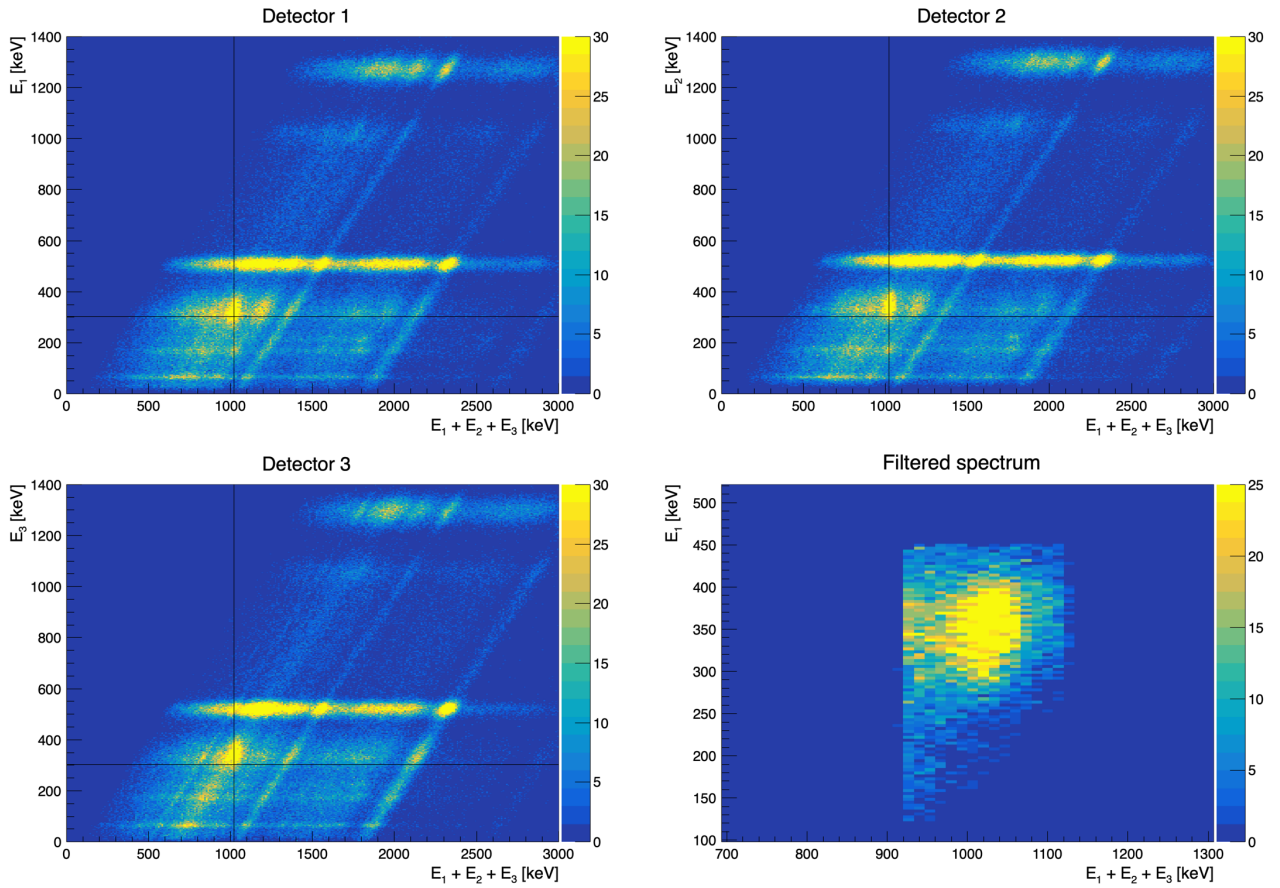

Figure 10: 2D histograms of the energy deposited in one detector E_i in function of the total energy E_{sum}. The black lines indicate the point that corresponds to $E_i = 340$ keV and $E_{sum} = 1022$ keV, hence to potential three photons events. In the last panel an example of a filtered spectrum is reported.

The temporal distribution of events was studied by analyzing the acquired TAC spectrum. We obtained the spectrum reported in Figure 11 (right). Fitting the right tail with an exponential function in the form $f(x) = a \cdot e^{bx}$, it's possible to estimate the characteristic parameters of the decay, as described in Section 6.2. The following parameters are found:

$$b = (-0.41 \pm 0.08)\ \text{ns}^{-1} \implies \tau = (2.5 \pm 0.5)\ \text{ns}$$

It's crucial to stress that we do not have a sample that allows us to perform an accurate interpolation procedure, therefore the results we obtained are to be considered approximate. Nevertheless, looking at the right plot of Figure 11, we can infer that the ortho-Positronium has a longer lifetime than the para-Positronium (indeed there's a greater amount of events that deviate from the gaussian trend). The experimental value does not agree with the theoretical one (∼142 ns in a vacuum). This is probably due to a series of aspects:

- The positronium lifetime depends on the material it interacts with;
- even if the TAC detects a valid event we cannot be sure that the START and STOP came from the same decay;
- the timing resolution of the detector may have an influence as well.

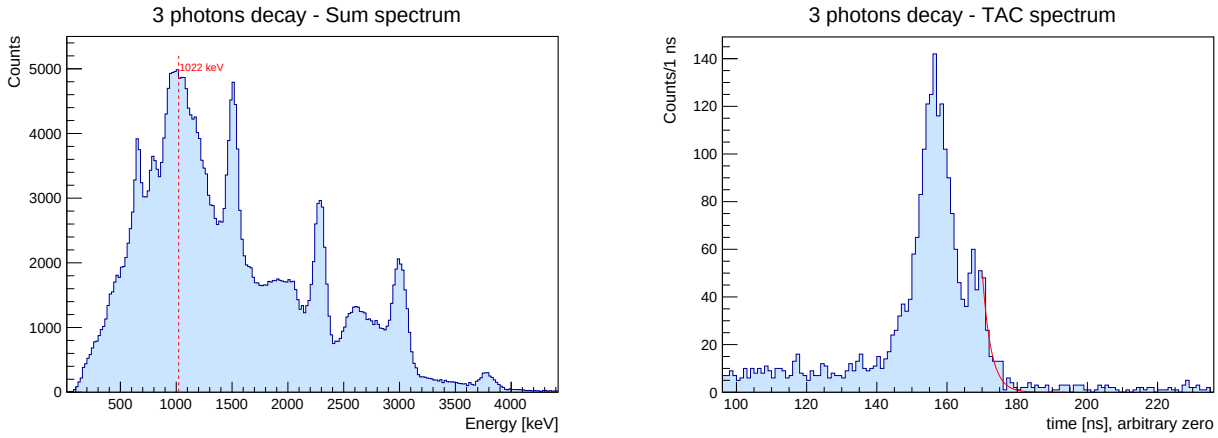

Figure 11: Left: Sum spectrum for three gammas decay. Right: TAC spectrum for three gammas decay, with exponential fit (red line).

8 Branching ratio and corrections

The aim of this section is to estimate the ratio between the 2γ and 3γ events; in order to do so, we take into consideration the rate of the two acquisitions, applying filters to select only relevant events but using the spectra recorded without the D4 coincidence: we obtain $f_{2\gamma} = (2605 \pm 7)$ Hz and $f_{3\gamma} = (0.150 \pm 0.001)$ Hz (uncertainties computed assuming a Poisson distribution). In order to correct the results obtained from the analysis of the 2γ and 3γ decays, some considerations have been made in terms of the setup geometry and of the detectors efficiency. The detection of the photon indeed depends on the solid angle subtended by the detector and seen by the ^{22}Na source. In good approximation we consider circular detectors with a radius r$\sim$ 5 cm and the distance source-detectors as d$\sim$ 15 cm. Therefore, we're assuming that the decays occur at the center of a sphere of radius d with the detectors on its surface.

- As far as the 2γ decay is concerned, due to momenta conservation, if a photon is detected by D1, the second one is collinear and detected as well by D2. This implies that the probability of detecting the two photons can be computed as the ratio between the sum of the two detectors areas and the area of the spherical surface, assuming the emission to be isotropic:

$$P_{2\gamma} = \frac{2\pi r^2}{4\pi d^2} \tag{4}$$

- The 3γ decay is more complicated because photons do not have a fixed energy but their spectra are continuous. For this reason, the calculation of the probability has been performed only in the simple case of equal angles between detectors and it has been found as the compound probability of the one of the single detectors. Similarly to the previous case, the first photon is detected by one of the three detectors with a probability that is equal to: $P_1 = \frac{3\pi r^2}{4\pi d^2}$. The second photon then will be revealed by one of the detectors left, with $P_2 = \frac{2\pi r^2}{4\pi d^2}$. The third photon has the constraint to be coplanar with respect to the other two, so it may be reasonable to assume that only one third of the plane is available for its detection. As result of this, the probability might be in the form $P_3 \sim 3 \cdot \frac{2r}{2\pi d}$. It then results:

$$P_{3\gamma} = P_1 \cdot P_2 \cdot P_3 \sim \frac{9r^5}{8\pi d^5} \tag{5}$$

These results are used to normalize the frequency of each decay in order to calculate the ratio R between them:

$$\mathrm{R} = \frac{3\gamma}{2\gamma} = \frac{f_{3\gamma} P_{2\gamma}}{f_{2\gamma} P_{3\gamma}} \sim \frac{1}{450} \sim 0.002 \tag{6}$$

The experimental value turns out to be slightly lower than the theoretical one, i.e. $\frac{1}{373} \sim 0.003$. This discrepancy could be due to different approximations introduced in the calculations: firstly, the model used to describe the geometry of the system is likely to be oversimplified; secondly, the distance detectors-source was not accurately measured.

8.1 Detector intrinsic efficiency

An additional correction factor can be added taking into account the detector intrinsic efficiency, hence we have:

$$R^* = R \cdot \frac{\varepsilon^2_{511\ \text{keV}}}{\varepsilon^3_{340\ \text{keV}}} \sim R \cdot 0.96$$

where $\varepsilon_{340\ \text{keV}}$ and $\varepsilon_{511\ \text{keV}}$ are the detectors intrinsic efficiency at the energies of interest, with the number of emitted gammas as exponent. Looking at Figure 12, the following values are retrieved[4]: $\varepsilon_{340\ \text{keV}} \sim 0.98$ and $\varepsilon_{511\ \text{keV}} \sim 0.95$. We can then conclude that the detectors efficiency does not make a significant contribution.

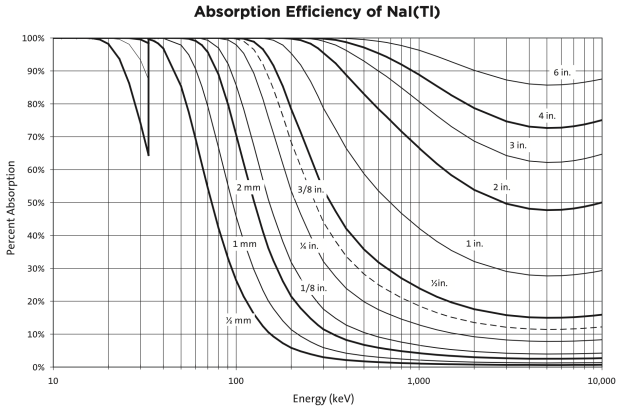

Figure 12: NaI(Tl) efficiency in function of energy, for certain values of thickness.

9 Conclusions

To sum up and give some conclusion about the experimental results, we can state that:

- The acquired spectra follow the expected trend; the energy calibration was successful, highlighting peaks at the right energy values and thus resulting in a comparable resolution for the four detectors; the TAC calibration confirmed the expected linear response of the module. For what concerns the dead time analysis, it was found that this correction is significant at high rates but can be neglected at low rates, i.e. for the 2γ and 3γ acquisitions.
- as far as the temporal distribution is concerned, the estimated lifetime of the para-Positronium shows a good agreement with the theoretical value, whereas the one of the ortho-Positronium is significantly different. This last inconsistency can be explained assuming a wide range of potential causes, among which the interaction with the material as well as the low statistics of the acquisition;
- various attempts were made to suppress multiple scattering and accidental coincidences, to avoid the misidentification of events and to isolate only the relevant ones. Thanks to a filtering procedure and geometrical considerations we obtained an branching ratio between 3γ and 2γ decays equal to $\sim \frac{1}{450}$. Although this experimental outcome is not in perfect agreement with the theoretical expectations, we managed to get a result that is comparable and consistent in order of magnitude.

[4]Taken from *Efficiency Calculations for Selected Scintillators*